



14 **Abstract.** Flash drought is characterized by its rapid onset and arouses wide concerns
15 due to its devastating impacts on the environment and society without sufficient early
16 warnings. The increasing frequency of flash drought in a warming climate highlights
17 the importance of understanding its impact on terrestrial ecosystems. Previous studies
18 investigated the vegetation dynamics during several extreme cases of flash drought,
19 but there is no quantitative assessment on how fast the carbon fluxes respond to flash
20 drought based on decade-long records with different climates and vegetation
21 conditions. Here we identify flash drought events by considering decline rate of soil
22 moisture and the drought persistency, and detect the response of ecosystem carbon
23 and water fluxes to flash drought during its onset and recovery stages based on
24 observations at 34 FLUXNET stations from grasslands to forests. Corresponding to
25 the sharp decline in soil moisture, gross primary productivity (GPP) drops below its
26 normal conditions in the first 16 days and reduces to its minimum within 24 days for
27 more than 50% of the 165 identified flash drought events, and savannas show highest
28 sensitivity to flash drought. Water use efficiency increases for forests but decreases
29 for cropland and savanna during the recovery stage of flash droughts. These results
30 demonstrate the rapid responses of vegetation productivity and physiological
31 adaptation for forest ecosystems to flash drought.

32 **Keywords:** Flash drought; GPP; Soil moisture; Water use efficiency; FLUXNET



33 **1. Introduction**

34 Terrestrial ecosystems play a key role in the global carbon cycle and absorb
35 about 30% of anthropogenic carbon dioxide emissions during the past five decades
36 (Le Quéré et al., 2018). With more climate extremes (e.g. drought, heat wave) in a
37 warming climate, the rate of land carbon uptake is highly uncertain regardless of the
38 fertilization effect of rising atmospheric carbon dioxide (Green et al., 2019;
39 Reichstein et al., 2013; Xu et al., 2019). Terrestrial ecosystems can even turn to
40 carbon source in some extreme drought events (Ciais et al., 2005). Record-breaking
41 drought events have caused enormous reduction of the ecosystem gross primary
42 productivity (GPP), such as the European 2003 drought (Ciais et al., 2005; Reichstein
43 et al., 2007), USA 2012 drought (Wolf et al., 2016), China 2013 drought (Xie et al.,
44 2016; Yuan et al., 2016), Southern Africa 2015/16 drought (Yuan et al., 2017) and
45 Australia Millennium drought (Banerjee et al., 2013). The 2012 summertime drought
46 in USA was classified as flash drought with rapid intensification and insufficient early
47 warning, which caused 26% reduction in crop yield (Hoerling et al., 2014; Otkin et al.,
48 2016). Flash drought has aroused wide concerns for its unusually rapid development
49 and detrimental effects (Basara et al., 2019; Christian et al., 2019; Ford & Labosier,
50 2017; Nguyen et al., 2019; Otkin et al., 2018; Yuan et al., 2015; Yuan et al., 2017;
51 Yuan et al., 2019b). Despite the increasing occurrence and clear ecological impacts of
52 flash droughts, our understanding of their impacts on carbon uptake in terrestrial
53 ecosystems remains incomplete.

54 Recent studies assessed the impact of flash drought on vegetation including the



55 2012 central USA flash drought and the 2017 northern USA flash drought. For
56 instance, Otkin et al. (2016) used the evaporative stress index (ESI) to detect the onset
57 of the 2012 central USA flash drought, and found the decline in ESI preceded the
58 drought according to the United States Drought Monitor. He et al. (2019) assessed the
59 impacts of the 2017 northern USA flash drought on vegetation productivity based on
60 GOME-2 solar-induced fluorescence (SIF) and satellite-based evapotranspiration in
61 the US Northern plains. Otkin et al. (2019) examined the evolution of vegetation
62 conditions using LAI from MODIS during the 2015 flash drought over the
63 South-Central United States and found that the LAI decreased after the decline of soil
64 moisture. However, previous impact studies only focused on a few extreme flash
65 drought cases without explicit definition of flash drought events. As the baseline
66 climate is changing (Yuan et al., 2019b), it is necessary to systematically investigate
67 the response of terrestrial carbon and water fluxes to flash drought events based on
68 long-term records rather than one or two extreme cases.

69 In fact, there are numerous studies on the influence of drought on ecosystem
70 productivity (Ciais et al., 2005; Stocker et al., 2018; Stocker et al., 2019). It is found
71 that understanding the coupling of water-carbon fluxes during drought is the key to
72 revealing the adaptation and response mechanisms of vegetation to water stress
73 (Boese et al., 2019; Nelson et al., 2018). Water use efficiency (WUE) is the metric for
74 understanding the trade-off between carbon assimilation and water loss through
75 transpiration (Beer et al., 2009; Cowan and Farquhar, 1977; Zhou et al., 2014, 2015),
76 and it is influenced by environmental factors including atmospheric dryness and soil



77 moisture limitations (Boese et al., 2019). Although WUE has been widely studied for
78 seasonal to decadal droughts, few studies have investigated WUE during flash
79 droughts that usually occur at sub-seasonal time scale.

80 In this paper, we address the ecological impact of flash droughts through
81 analyzing FLUXNET decade-long observations of CO₂ and water fluxes. The specific
82 goals are to (1) examine the response of carbon and water fluxes to flash droughts
83 from the onset to the recovery stages, and (2) investigate how WUE changes during
84 flash drought for different ecosystems. The methodology proposed by Yuan et al.
85 (2019b) enables the analysis of the flash drought with characteristics of duration,
86 frequency, and intensity in the historical observations. All the flash drought events
87 occurred at the FLUXNET stations are selected to investigate the response of carbon
88 fluxes and WUE. More than 10-year records of soil moisture, carbon and water fluxes
89 are available (Baldocchi et al., 2002), which makes it possible to assess the response
90 of vegetation to flash droughts by considering different climates and ecosystem
91 conditions.

92 **2. Data and Methods**

93 **2.1 Data**

94 FLUXNET2015 provides daily hydrometeorological variables including
95 precipitation, temperature, saturation vapor pressure deficit (VPD), soil moisture (sm),
96 evapotranspiration (ET) inferred from latent heat, and carbon fluxes including GPP.
97 We use GPP data based on night-time partitioning method (GPP_NT_VUT_REF).
98 Considering most sites only measure the surface soil moisture, here we use daily soil



99 moisture measurements mainly at the depth of 5-10 cm averaged from half-hourly
100 data. All daily hydrometeorological variables and carbon fluxes are summed to 8-day
101 time scale to study the flash drought impact. We select 34 sites from FLUXNET 2015
102 dataset (Table 1), where the periods of observations are no less than 10 years ranging
103 from 1996 to 2014, and the rates of missing data are lower than 5%. The FLUXNET
104 observations include 12 evergreen needleleaf forest sites (ENF), 5 deciduous
105 broadleaf forests (DBF) and 6 crop sites (CROP; 5 rain-fed sites and 1 irrigated site)
106 etc. The detailed information is listed in Table 1. Here we select three flash drought
107 cases at different ecosystems including ENF (FI-Sod site), savanna (SAV; US-SRM
108 site) and DBF (IT-Col site) to show the response of vegetation to flash droughts.

109 **2.2 Methods**

110 **2.2.1 Definition of flash drought events**

111 The definition of flash drought should account for both its rapid intensification
112 and the drought conditions (Otkin et al., 2018; Yuan et al., 2019b). Here we used soil
113 moisture percentile to identify flash drought according to Yuan et al. (2019b) and Ford
114 et al. (2017). Figure 1 shows the procedure for flash drought identification, including
115 five criteria to identify the rapid onset and recovery stages of flash drought. 1) Flash
116 drought starts when the 8-day mean soil moisture is less than the 40th percentile, and
117 the 8-day mean soil moisture prior to the starting time should be higher than 40th
118 percentile to ensure the transition from a non-drought condition. 2) The mean
119 decreasing rate of 8-day mean soil moisture percentile should be no less than 5% to
120 address the rapid drought intensification. 3) The 8-day mean soil moisture after the



121 rapid decline should be less than 20% in percentile, and the period from the beginning
122 to the end of the rapid decline is regarded as the onset stage of flash drought (those
123 within red dashed line in Figure 1). 4) If the mean decreasing rate is less than 5% in
124 percentile or the soil moisture percentile starts to increase, the flash drought enters
125 into the “recovery” stage, and the flash drought event (as well as the recovery stage)
126 ends when soil moisture recovers to above 20th percentile (those within blue dashed
127 line in Figure 1). The recovery stage is also crucial to assess the impact of flash
128 drought (Yuan et al., 2019b). 5) The minimum duration of a flash drought event is 24
129 days to exclude those dry spells that last for a too short period to cause any impacts,
130 and the maximum duration is limited to 2 months to separate flash droughts from
131 traditional droughts (e.g., seasonal droughts).

132 Decade-long observations of 8-day mean soil moisture are used to calculate soil
133 moisture percentile with a moving window of 8-day before and 8-day after the target
134 8-day, resulting in at least 30 samples for deriving the cumulative distribution
135 function of soil moisture before calculating percentiles. For example, the soil moisture
136 percentile of June 22nd in 1998 is calculated by firstly ranking June 14th, June 22nd,
137 and June 30th soil moisture in all historical years (N samples) from lowest to highest,
138 identifying the rank of soil moisture of June 22nd, 1998 (e.g., M), and obtaining the
139 percentile as $M/N \times 100$. We focus on growing seasons during April-September for
140 sites in the North Hemisphere and October-March for sites in the South Hemisphere.

141 **2.2.2 Response time of GPP to flash drought**

142 Drought has a large influence on ecosystem productivity through altering the plant



143 photosynthesis and ecosystem respiration (Beer et al., 2010; Green et al., 2019;
144 Heimann & Reichstein, 2008; Stocker et al., 2018). GPP dominates the global
145 terrestrial carbon sink and it would decrease due to stomatal closure and non-stomatal
146 limitations like reduced carboxylation rate and reduced active leaf area index (de la
147 Motte et al., 2019) under water stress. The negative anomalies of GPP during flash
148 drought are considered as the signal of ecological deterioration. Here, we use two
149 response time indices to investigate the relationship between flash drought and
150 ecological drought (Niu et al., 2018; Song et al., 2018; Vicente-Serrano et al., 2013): 1)
151 the response time of the first occurrence of negative standardized GPP anomaly
152 ($SGPPA = \frac{GPP - \mu_{GPP}}{\sigma_{GPP}}$, where μ_{GPP} and σ_{GPP} are mean and standard deviation of the
153 time series of GPP at the same dates as the target 8-days for all years, which can
154 remove the influence of seasonality. For instance, all Apr 1-8 during 1996-2014 would
155 have a μ_{GPP} and a σ_{GPP} , and Apr 9-16 would have another μ_{GPP} and another σ_{GPP} ,
156 and so on), which is the lag time between the start of flash drought and the time when
157 SGPPA becomes negative during flash drought period; and 2) the response time of
158 occurrence of minimum SGPPA, which is the lag time between the start of flash
159 drought and the time when SGPPA decreases to its minimum values during the flash
160 drought period. If the response time is 8 days for the first occurrence of negative
161 SGPPA, it means that the response of GPP starts at the beginning of flash drought (the
162 first time step of flash drought).

163 2.2.3 Water use efficiency

164 Carbon assimilation and transpiration are coupled by stomates under the



165 influence of water and energy conditions (Boese et al., 2019; Huang et al., 2016;
166 Nelson et al., 2018). Plants face a tradeoff at the level of the stomata to fix carbon
167 through photosynthesis at the cost of water losses through transpiration. WUE
168 quantifies the trade-off, which is defined as the assimilated amount of carbon per unit
169 of water loss. At the ecosystem scale, WUE is the ratio of GPP over ET (Cowan and
170 Farquhar, 1977). Drought would cause stomatal closure and non-stomatal adjustments
171 in biochemical functions thus altering the coupling between GPP and ET. Underlying
172 WUE (uWUE) is calculated as $GPP \times \sqrt{VPD} / ET$ considering the nonlinear
173 relationship between GPP, VPD and ET (Zhou et al., 2014). uWUE is supposed to
174 reflect the relationship of photosynthesis-transpiration via stomatal conductance at the
175 ecosystem level by considering the effect of VPD on WUE (Beer et al., 2009; Boese
176 et al., 2019; Zhou et al., 2014, 2015). WUE varies under the influence of VPD on
177 canopy conductance (Beer et al., 2009; Tang et al., 2006), whereas uWUE is
178 considered to remove this effect and be more directly linked with the relationship
179 between environmental conditions (e.g., soil moisture) and plant conditions (e.g.,
180 carboxylation rate; Lu et al., 2018). The standardized anomalies of WUE and uWUE
181 are calculated the same as SGPPA, where different sites have different mean values
182 and standard deviations for different target 8-days to remove the spatial and temporal
183 inhomogeneity.

184 **3. Results**

185 **3.1 Identification of flash drought events at FLUXNET stations**

186 Based on FLUXNET data, we have identified 165 flash drought events with



187 durations longer than 24 days using soil moisture observations of 428 site years.
188 Figure 2a shows the distribution of the 34 sites with different vegetation types. The
189 number of flash drought ranged from 1 to 12 events among FLUXNET sites, and the
190 mean durations were from around 30 days to 60 days among FLUXNET sites
191 (Figures 2b and 2c). The frequency of flash drought shows great spatial heterogeneity
192 which may be associated with variability of soil moisture. If enough rainfall comes
193 after the flash drought, the soil moisture could recover to above 20% percentile.
194 Without enough rainfall for recovery, flash drought would ultimately develop into
195 longer and more severe drought (Wang and Yuan, 2018).

196 Figure 3 shows the standardized anomalies of temperature, precipitation, VPD,
197 and ET during different stages of flash drought. There is a slight reduction in
198 precipitation and increase in ET during 8 days prior to flash drought (Figure 3b&d).
199 During the onset of flash drought, the rapid drying of soil moisture is always
200 associated with a large precipitation deficits, and anomalously high temperature and
201 large VPD indicate increased atmospheric dryness (Ford et al., 2017; Koster et al.,
202 2019; Wang et al., 2016), which persist until the recovery stage. ET is close to normal
203 conditions thus enhancing the drying rate of soil moisture with less precipitation
204 supply during the onset stage (Figure 3b&d). However, ET starts to decrease during
205 the recovery stage because of the limitation from water availability, which alleviates
206 the drought condition. Sufficient precipitation occurs during the 8 days after flash
207 droughts to relieve the drought condition.

208 **3.2 Evolutions of carbon and water fluxes during flash drought events**



209 Figure 4 shows the evolutions of soil moisture percentile, standardized GPP and
210 ET anomalies during the flash droughts occurred in 2003 at FI-Sod site (Ciais et al.,
211 2005), 2004 at US-SRM site and 2007 at IT-Col site.

212 FI-Sod is covered by northern boreal Scots pine with mean annual temperature of
213 -1°C (Thum et al., 2007). 2003 summer drought over Europe accompanied by heat
214 wave caused enormous carbon losses with 30% reduction in GPP (Ciais et al., 2005),
215 and the drought outweighed heat wave for influencing the ecosystem (Reichstein et al.,
216 2007). The 2003 flash drought at FI-Sod occurred in the late of June and ended in the
217 early July although the soil moisture condition was still below the climatology (Figure
218 4a). During the 24-day flash drought, GPP and ET respond quickly to the rapid soil
219 moisture drying and recover to their normal conditions as soon as the drought relieves
220 (Figures 4b and 4c), which shows the resilience of evergreen needleleaf forest to
221 short-term drought. Negative ET anomaly (Figure 4c) precedes the onset of soil
222 moisture drought, indicating that the flash drought is mainly caused by rainfall deficit
223 (Figure 4a).

224 US-SRM site is in dry land savanna. Savanna covers 20% of the global land area
225 (Sankaran et al., 2005), and influences the terrestrial carbon sink significantly
226 (Ahlstrom et al., 2015). Soil moisture plays a crucial role in regulating carbon and
227 water fluxes in savanna regions (Scott et al., 2009; Williams & Albertson, 2004; Wolf
228 et al., 2016), and there is a large variability of soil moisture at US-SRM. Soil moisture
229 percentile declined from 33% to 5% in 8 days and stayed below 20% for 8 days
230 (Figure 4d). The rapid decline in soil moisture is mainly from rainfall deficits because



231 the evapotranspiration process is limited by soil water in semiarid savanna region.
232 GPP and ET both decrease with the decline in soil moisture (Figures 4e and 4f), and
233 the negative anomalies persist even after the flash drought. As there is not enough
234 rainfall to alleviate soil moisture drought, the vegetation damage continues (Figure
235 4e).

236 The flash drought lasted for 56 days in 2007 at IT-Col site and propagated into a
237 long-term drought due to the persistence of precipitation deficits. IT-Col is in
238 deciduous broadleaf forest with relatively humid climate (Van Dijk & Dolman, 2004).
239 There is a lag time of 8 days between the responses of GPP and ET to flash drought
240 (Figures 4h and 4i), which is because that the positive evapotranspiration anomaly at
241 the onset of flash drought (30th in June) is driven by higher temperature and VPD.
242 GPP and ET are below the climatology during flash drought, indicating the
243 degradation in vegetation under water stress. The whole reduction of ET during flash
244 drought is relatively small compared with GPP, indicating the decoupling between
245 water and carbon fluxes.

246 In short, both GPP and ET fluxes reduce rapidly in responding to the sharp
247 decline in soil moisture, although the reduction depends on environmental conditions
248 and vegetation characteristics (Vicente-Serrano et al., 2013).

249 **3.3 Climatological statistics of the response time of GPP to flash drought**

250 By analyzing all the 165 flash drought events across 34 FLUXNET sites, we find
251 that negative GPP anomalies occur during 81% of the flash drought events. Figures 5a
252 and 5b show the probability distributions of the response time of GPP to flash drought



253 for the first occurrence of negative SGPPA and the minimum negative value of
254 SGPPA, respectively. The first occurrences of negative SGPPA are concentrated
255 during the first 24 days, and for 57% flash droughts, GPP starts to respond to flash
256 drought within 16 days (Figure 5a). The occurrences of minimum value of SGPPA
257 rise sharply at the beginning of flash drought, and reach the peak during 17-24 days,
258 and then slow down (Figure 5b), which is similar to the decline in soil moisture.
259 Although the first occurrences of negative SGPPA mainly occur in onset stage, GPP
260 would continue to decrease in recovery stages for 60% of flash drought events. The
261 time for soil moisture reaching its minimum is concentrated during 9-16 days since
262 the occurrence of flash drought, preceding the minimum GPP by about 8 days. Large
263 decreases in soil moisture percentiles are during the first 16 days of flash drought
264 (Figure 5c), while large decrease in GPP occurs during 9-24 days (Figure 5d).

265 Different types of vegetation including herbaceous plants and woody plants all
266 react to flash drought in the early stage (Figures 6). Among them, savanna shows the
267 fastest reaction to water stress (Figure 6a&6f), with 63% events showing vegetation
268 response concurrently with flash drought onset and ultimately 88% events showing
269 impaired vegetation photosynthesis. The result is consistent with the high
270 vulnerability of vegetation in semiarid regions (Vicente-Serrano et al., 2013; Zeng et
271 al., 2018). The decline rates in soil moisture show differences among different
272 vegetation types during flash drought, which are related to soil texture, vegetation
273 cover and climates.

274 **3.4 WUE under soil moisture stress**



275 Figure 7 shows the standardized anomalies of WUE and uWUE and their
276 components for different ecosystems during the onset and recovery stages of flash
277 drought. Evergreen broadleaf forest (EBF) and grassland (GRA) were excluded due to
278 insufficient flash drought cases. Here, we select 81% of flash drought events with
279 GPP declining down to its normal conditions to analyze the interactions between
280 carbon and water fluxes. WUE is stable during the onset stage except for croplands
281 and mixed forests (MF), whereas uWUE increases for all ecosystems (Figure 7a). For
282 croplands, both GPP and ET decrease, and the decline in WUE is related with a
283 greater reduction in GPP relative to ET (Figure 7c&e). The positive anomalies of
284 uWUE are correlated with decrease in ET/\sqrt{VPD} mainly induced by the high VPD.
285 Increasing VPD and deficits in soil moisture would decrease canopy conductance
286 (Grossiord et al., 2020) but not GPP for MF and ENF. During the onset stage, GPP
287 and ET reduce only for savannas, croplands, and DBF, and the magnitudes of GPP
288 and ET reduction are highest for savannas. But for recovery stage, GPP and ET show
289 significant reductions except for MF, and the responses of WUE and uWUE are
290 different between herbaceous plants (savannas and croplands) and forests (MF, DBF,
291 and ENF), where WUE and uWUE decrease significantly for savannas and croplands
292 but increase slightly for forests (Figure 7b). The decrease in GPP during recovery
293 stage is not only related to the reduction in canopy conductance, but also the decrease
294 in uWUE under drought for savannas and croplands which is possibly influenced by
295 suppressed state of enzyme and reduced mesophyll conductance (Flexas et al., 2012).
296 The average soil moisture conditions are 11% in percentile for recovery stage but 18%



297 for onset stage. So, drier soil moisture in the recovery stage exacerbates ecological
298 response. Figure 7b also shows the higher WUE and uWUE for forests, which
299 indicates their higher resistance to flash drought than herbaceous plants during
300 recovery stage.

301 **4. Discussion**

302 Previous studies detected the vegetation response for a few extreme drought cases
303 without a specific definition of flash drought from a climatological perspective (Otkin
304 et al., 2016; He et al., 2019). Moreover, less attention has been paid to the coupling
305 between carbon and water fluxes during flash drought events. This study investigates
306 the response of carbon and water fluxes to flash drought based on decade-long
307 FLUXNET observations. The responses vary across different phases of flash drought,
308 and different ecosystems have different responses, which provide implications for
309 eco-hydrological modeling and prediction.

310 **4.1 The responses of carbon and water fluxes to flash droughts**

311 Based on 165 flash drought events identified using soil moisture from
312 decade-long FLUXNET observations, the response of GPP to flash drought is found
313 to be quite rapid. For more than half of the 165 flash drought events, the GPP drops
314 below its normal conditions during the first 16 days and reaches its maximum
315 intensity within 24 days. Eventually, 81% of flash drought events cause negative
316 ecological impacts on GPP. During the drought period, plants would close their
317 stomata to minimize water loss through decreasing canopy conductance, which in turn
318 leads to a reduction in carbon uptake. High VPD further reduces canopy conductance



319 during flash drought. The suppression of GPP and ET is more obvious for flash
320 drought recovery stage than the onset stage. The discrepancy of GPP responses
321 between different phases of flash drought may result from 1) soil moisture conditions
322 which are drier during the recovery stage, and 2) the damaged physiological
323 functioning for specific vegetation types. The anomalies of uWUE for ecosystems are
324 always positive or unchanged during flash drought except for croplands and savannas
325 during recovery stage. The decrease in canopy conductance would limit
326 photosynthetic rate, however, the increase of uWUE indicates adaptative regulations
327 of ecosystem physiology which is consistent with Beer et al. (2009). uWUE is higher
328 than WUE during onset stage of flash drought, which is due to the decreased
329 conductance under increased VPD. However, there is no obvious difference between
330 WUE and uWUE during recovery stage, which indicates that photosynthesis is less
331 sensitive to stomatal conductance and may be more correlated with limitations of
332 biochemical capacity (Flexas et al., 2012; Grossiord et al., 2020).

333 This study is based on the sites that are mainly distributed over North America
334 and Europe. It is necessary to investigate the impact of flash drought on vegetation
335 over other regions with different climates and vegetation conditions. In addition, this
336 study used in-situ surface soil moisture at FLUXNET stations to detect vegetation
337 response due to the lack of soil moisture observations at deep soil layers. There would
338 be more significant ecological responses to flash drought identified through using
339 root-zone soil moisture because of its close link with vegetation dynamics.

340 **4.2 Variation in ecological responses across vegetation types**



341 The responses of GPP, ET and WUE to flash drought vary among different
342 vegetation types. The decline in GPP and ET only occurs across croplands and
343 savannas during onset stage. For most forests, the deterioration of photosynthesis and
344 ET appears during the recovery stage with higher WUE and uWUE. For croplands
345 and savannas, both WUE and uWUE decrease during the recovery stage. The positive
346 anomalies of WUE and uWUE for forests show the adaptation of vegetation to flash
347 drought from physiological perspective. Xie et al. (2016) pointed out that WUE and
348 uWUE for a subtropical forest increased during the 2013 summer drought in southern
349 China. The increased WUE in forest sites and unchanged WUE in grasslands were
350 also found in other studies for spring drought (Wolf et al., 2013). In general,
351 herbaceous plants are more sensitive to flash drought than forests, especially for
352 savannas.

353 **4.3 Potential implications for ecosystem modelling**

354 The study reveals the profound impact of flash droughts on ecosystem through
355 analyzing eddy covariance observations. It is found that the responses of carbon and
356 water exchanges are quite distinguishing for forests and herbaceous plants. For the
357 ecosystem modeling, the response of stomatal conductance under soil moisture stress
358 has been addressed in previous studies (Wilson et al., 2000), but there still exists
359 deficiency to capture the impacts of water stress on carbon uptake (Keenan et al.,
360 2009), which is partly due to the different responses across species. Incorporating
361 physiological adaptations to drought in ecosystem modeling especially for forests
362 would improve the simulation of the impact of drought on the terrestrial ecosystems.



363 5. Conclusion

364 This study presents how carbon and water fluxes respond to flash drought during
365 onset and recovery stages through analyzing decade-long observations from
366 FLUXNET. Ecosystems show high sensitivity of GPP to flash drought especially for
367 savannas, and GPP starts to respond to flash droughts within 16 days for more than
368 half of the flash drought events. However, the responses of WUE and uWUE vary
369 across vegetation types. Positive WUE and uWUE anomalies for forests during the
370 recovery stage indicate the physiological adaptation to flash drought through
371 non-stomatal regulations, whereas WUE and uWUE decrease for croplands and
372 savannas during the recovery stage. For now, the main concern about the ecological
373 impact of flash drought is concentrated on the period of flash drought and the legacy
374 effects of flash drought are not involved. It still needs more efforts to study the
375 subsequent effects of flash droughts which would contribute to assessing the
376 accumulated ecological impacts of flash drought. Nevertheless, this study highlights
377 the rapid response of vegetation productivity to soil moisture dynamics at
378 sub-seasonal timescale, and different responses of water use efficiency across
379 ecosystems during the recovery stage of flash droughts, which complements previous
380 studies on the sensitivity of vegetation to extreme drought at longer time scale.
381 Understanding the response of carbon fluxes and the coupling between carbon and
382 water fluxes to drought might help assessing the resistance and resilience of
383 vegetation to drought.

384



385 **Acknowledgements**

386 This work was supported by National Natural Science Foundation of China
387 (41875105), National Key R&D Program of China (2018YFA0606002) and the
388 Startup Foundation for Introducing Talent of NUIST. The data used in this study are
389 all from FLUXNET 2015 (<https://fluxnet.fluxdata.org/data/fluxnet2015-dataset/>).

390

391 **Data availability statement**

392 Carbon fluxes and hydrometeorological variables from FLUXNET2015 are available
393 through <https://fluxnet.fluxdata.org/data/fluxnet2015-dataset/>.



394 **References**

- 395 Atjay, G. L., Ketner, P. and Duvigneaud, P.: Terrestrial primary production and
396 phytomass, in *The Global Carbon Cycle: SCOPE 13*, John Wiley, Hoboken, N. J.,
397 129–182, 1979
- 398 Ahlstrom, A., Raupach, M. R., Schurgers, G., Smith, B., Arneeth, A., Jung, M.,
399 Reichstein, M., Canadell, J. G., Friedlingstein, P., Jain, A. K., Kato, E., Poulter,
400 B., Sitch, S., Stocker, B. D., Viovy, N., Wang, Y. P., Wiltshire, A., Zaehle, S. and
401 Zeng, N.: The dominant role of semi-arid ecosystems in the trend and variability
402 of the land CO₂ sink, *Science*, 348(6237), 895–899,
403 <https://doi.org/10.1126/science.aaa1668>, 2015.
- 404 Baldocchi, D., Wilson, K., Valentini, R., Law, B., Munger, W., Davis, K., Wofsy, S.,
405 Pilegaard, K., Goldstein, A., Falge, E., Vesala, T., Hollinger, D., Running, S.,
406 Fuentes, J., Katul, G., Gu, L., Verma, S., Paw, K. T., Malhi, Y., Anthoni, P.,
407 Oechel, W., Schmid, H. P., Bernhofer, C., Meyers, T., Evans, R., Olson, R. and
408 Lee, X.: FLUXNET: A New Tool to Study the Temporal and Spatial Variability
409 of Ecosystem–Scale Carbon Dioxide, Water Vapor, and Energy Flux Densities,
410 *Bull. Am. Meteorol. Soc.*, 82(11), 2415–2434, <https://doi.org/10.1175/1520-0477>,
411 2002.
- 412 Banerjee, O., Bark, R., Connor, J. and Crossman, N. D.: An ecosystem services
413 approach to estimating economic losses associated with drought, *Ecol. Econ.*, 91,
414 19–27, <https://doi.org/10.1016/j.ecolecon.2013.03.022>, 2013.
- 415 Basara, J. B., Christian, J. I., Wakefield, R. A., Otkin, J. A., Hunt, E. H. H. and Brown,



- 416 D. P.: The evolution, propagation, and spread of flash drought in the Central
417 United States during 2012, *Environ. Res. Lett.*, 14(8),
418 <https://doi.org/10.1088/1748-9326/ab2cc0>, 2019.
- 419 Beer, C., Ciais, P., Reichstein, M., Baldocchi, D., Law, B. E., Papale, D., Soussana, J.
420 F., Ammann, C., Buchmann, N., Frank, D., Gianelle, D., Janssens, I. A., Knohl,
421 A., Köstner, B., Moors, E., Rouspard, O., Verbeeck, H., Vesala, T., Williams, C.
422 A. and Wohlfahrt, G.: Temporal and among-site variability of inherent water use
423 efficiency at the ecosystem level, *Global Biogeochem. Cycles*, 23(2), 1–13,
424 <https://doi.org/10.1029/2008GB003233>, 2009.
- 425 Beer, C., Reichstein, M., Tomelleri, E., Ciais, P., Jung, M., Carvalhais, N., Rödenbeck,
426 C., Arain, M. A., Baldocchi, D., Bonan, G. B., Bondeau, A., Cescatti, A., Lasslop,
427 G., Lindroth, A., Lomas, M., Luysaert, S., Margolis, H., Oleson, K. W.,
428 Rouspard, O., Veenendaal, E., Viovy, N., Williams, C., Woodward, F. I. and
429 Papale, D.: Terrestrial gross carbon dioxide uptake: Global distribution and
430 covariation with climate, *Science*, 329(5993), 834–838,
431 <https://doi.org/10.1126/science.1184984>, 2010.
- 432 Boese, S., Jung, M., Carvalhais, N., Teuling, A. J. and Reichstein, M.: Carbon-water
433 flux coupling under progressive drought, *Biogeosciences*, 16(13), 2557–2572,
434 <https://doi.org/10.5194/bg-16-2557-2019>, 2019.
- 435 Cowan, I. R. and Farquhar, G. D.: Stomatal function in relation to leaf metabolism
436 and environment, in *Integration of Activity in the Higher Plant*, edited by D. H.
437 Jennings, Cambridge Univ. Press, Cambridge, U. K., 471–505, 1977



- 438 Christian, J. I., Basara, J. B., Otkin, J. A., Hunt, E. D., Wakefield, R. A., Flanagan, P.
439 X. and Xiao, X.: A methodology for flash drought identification: Application of
440 flash drought frequency across the United States, *J. Hydrometeorol.*, 20(5), 833–
441 846, <https://doi.org/10.1175/JHM-D-18-0198.1>, 2019.
- 442 Ciais, P., Reichstein, M., Viovy, N., Granier, A., Ogée, J., Allard, V., Aubinet, M.,
443 Buchmann, N., Bernhofer, C., Carrara, A., Chevallier, F., De Noblet, N., Friend,
444 A. D., Friedlingstein, P., Grünwald, T., Heinesch, B., Keronen, P., Knohl, A.,
445 Krinner, G., Loustau, D., Manca, G., Matteucci, G., Miglietta, F., Ourcival, J. M.,
446 Papale, D., Pilegaard, K., Rambal, S., Seufert, G., Soussana, J. F., Sanz, M. J.,
447 Schulze, E. D., Vesala, T. and Valentini, R.: Europe-wide reduction in primary
448 productivity caused by the heat and drought in 2003, *Nature*, 437(7058), 529–
449 533, <https://doi.org/10.1038/nature03972>, 2005.
- 450 de la Motte, L. G., Beauclaire, Q., Heinesch, B., Cuntz, M., Foltýnová, L., Šigut, L.,
451 Kowalska, N., Manca, G., Ballarin, I. G., Vincke, C., Roland, M., Ibrom, A.,
452 Lousteau, D., Siebicke, L. and Longdoz, B.: Non-stomatal processes reduce
453 gross primary productivity in temperate forest ecosystems during severe edaphic
454 drought, *Philos. Trans. R. Soc. B*, <https://doi.org/10.1098/RSTB-2019-0527>,
455 2019.
- 456 Flexas, J., Barbour, M. M., Brendel, O., Cabrera, H. M., Carriqui í M., D áz-Espejo, A.,
457 Douthe, C., Dreyer, E., Ferrio, J. P., Gago, J., Gall é A., Galm és, J., Kodama, N.,
458 Medrano, H., Niinemets, Ü., Peguero-Pina, J. J., Pou, A., Ribas-Carbó M.,
459 Tomás, M., Tosens, T. and Warren, C. R.: Mesophyll diffusion conductance to



- 460 CO₂: An unappreciated central player in photosynthesis, *Plant Sci.*, 193–194,
461 70–84, <https://doi.org/10.1016/j.plantsci.2012.05.009>, 2012.
- 462 Ford, T. W. and Labosier, C. F.: Meteorological conditions associated with the onset
463 of flash drought in the Eastern United States, *Agric. For. Meteorol.*, 247(April),
464 414–423, <https://doi.org/10.1016/j.agrformet.2017.08.031>, 2017.
- 465 Ford, T. W., McRoberts, D. B., Quiring, S. M. and Hall, R. E.: On the utility of in situ
466 soil moisture observations for flash drought early warning in Oklahoma, USA,
467 *Geophys. Res. Lett.*, 42(22), <https://doi.org/10.1002/2015GL066600>, 2015.
- 468 Green, J. K., Seneviratne, S. I., Berg, A. M., Findell, K. L., Hagemann, S., Lawrence,
469 D. M. and Gentine, P.: Large influence of soil moisture on long-term terrestrial
470 carbon uptake, *Nature*, 565(7740), 476–479,
471 <https://doi.org/10.1038/s41586-018-0848-x>, 2019.
- 472 Grossiord, C., Buckley, T. N., Cernusak, L. A., Novick, K. A., Poulter, B., Siegwolf, R.
473 T. W., Sperry, J. S. and McDowell, N. G.: Plant responses to rising vapor
474 pressure deficit, *New Phytol.*, <https://doi.org/10.1111/nph.16485>, 2020.
- 475 He, M., Kimball, J. S., Yi, Y., Running, S., Guan, K., Jensco, K., Maxwell, B. and
476 Maneta, M.: Impacts of the 2017 flash drought in the US Northern plains
477 informed by satellite-based evapotranspiration and solar-induced fluorescence,
478 *Environ. Res. Lett.*, 14(7), 074019, <https://doi.org/10.1088/1748-9326/ab22c3>,
479 2019.
- 480 Heimann, M. and Reichstein, M.: Terrestrial ecosystem carbon dynamics and climate
481 feedbacks, *Nature*, 451(7176), 289–292, <https://doi.org/10.1038/nature06591>,



- 482 2008.
- 483 Hoerling, M., Eischeid, J., Kumar, A., Leung, R., Mariotti, A., Mo, K., Schubert, S.
484 and Seager, R.: Causes and predictability of the 2012 great plains drought, Bull.
485 Am. Meteorol. Soc., 95(2), 269–282,
486 <https://doi.org/10.1175/BAMS-D-13-00055.1>, 2014.
- 487 Huang, M., Piao, S., Zeng, Z., Peng, S., Ciais, P., Cheng, L., Mao, J., Poulter, B., Shi,
488 X., Yao, Y., Yang, H. and Wang, Y.: Seasonal responses of terrestrial ecosystem
489 water-use efficiency to climate change, Glob. Chang. Biol., 22(6), 2165–2177,
490 <https://doi.org/10.1111/gcb.13180>, 2016.
- 491 Keenan, T., Garc ía, R., Friend, A. D., Zaehle, S., Gracia, C. and Sabate, S.: Improved
492 understanding of drought controls on seasonal variation in mediterranean forest
493 canopy CO₂ and water fluxes through combined in situ measurements and
494 ecosystem modelling, Biogeosciences, 6(8), 1423–1444,
495 <https://doi.org/10.5194/bg-6-1423-2009>, 2009.
- 496 Koster, R. D., Schubert, S. D., Wang, H., Mahanama, S. P. and DeAngelis, A. M.:
497 Flash Drought as Captured by Reanalysis Data: Disentangling the Contributions
498 of Precipitation Deficit and Excess Evapotranspiration, J. Hydrometeorol., 20(6),
499 1241–1258, <https://doi.org/10.1175/jhm-d-18-0242.1>, 2019.
- 500 Nelson, J. A., Carvalhais, N., Migliavacca, M., Reichstein, M. and Jung, M.:
501 Water-stress-induced breakdown of carbon-water relations: Indicators from
502 diurnal FLUXNET patterns, Biogeosciences, 15(8), 2433–2447,
503 <https://doi.org/10.5194/bg-15-2433-2018>, 2018.



- 504 Nguyen, H., Wheeler, M. C., Otkin, J. A., Cowan, T., Frost, A. and Stone, R.: Using
505 the evaporative stress index to monitor flash drought in Australia, *Environ. Res.
506 Lett.*, 14(6), <https://doi.org/10.1088/1748-9326/ab2103>, 2019.
- 507 Niu, J., Chen, J., Sun, L. and Sivakumar, B.: Time-lag effects of vegetation responses
508 to soil moisture evolution: a case study in the Xijiang basin in South China,
509 *Stoch. Environ. Res. Risk Assess.*, 32(8), 2423–2432,
510 <https://doi.org/10.1007/s00477-017-1492-y>, 2018.
- 511 Otkin, J. A., Anderson, M. C., Hain, C., Mladenova, I. E., Basara, J. B. and Svoboda,
512 M.: Examining Rapid Onset Drought Development Using the Thermal Infrared–
513 Based Evaporative Stress Index, *J. Hydrometeorol.*, 14(4), 1057–1074,
514 <https://doi.org/10.1175/JHM-D-12-0144.1>, 2013.
- 515 Otkin, J. A., Anderson, M. C., Hain, C., Svoboda, M., Johnson, D., Mueller, R.,
516 Tadesse, T., Wardlow, B. and Brown, J.: Assessing the evolution of soil moisture
517 and vegetation conditions during the 2012 United States flash drought, *Agric. For.
518 Meteorol.*, 218–219, 230–242, <https://doi.org/10.1016/j.agrformet.2015.12.065>,
519 2016.
- 520 Otkin, J. A., Svoboda, M., Hunt, E. D., Ford, T. W., Anderson, M. C., Hain, C. and
521 Basara, J. B.: Flash droughts: A review and assessment of the challenges
522 imposed by rapid-onset droughts in the United States, *Bull. Am. Meteorol. Soc.*,
523 99(5), 911–919, <https://doi.org/10.1175/BAMS-D-17-0149.1>, 2018.
- 524 Otkin, J. A., Zhong, Y., Hunt, E. D., Basara, J., Svoboda, M., Anderson, M. C. and
525 Hain, C.: Assessing the Evolution of Soil Moisture and Vegetation Conditions



526 during a Flash Drought–Flash Recovery Sequence over the South-Central United
527 States, J. Hydrometeorol., 20(3), 549–562,
528 <https://doi.org/10.1175/jhm-d-18-0171.1>, 2019.

529 Quéré C., Andrew, R., Friedlingstein, P., Sitch, S., Hauck, J., Pongratz, J., Pickers, P.,
530 Ivar Korsbakken, J., Peters, G., Canadell, J., Arneeth, A., Arora, V., Barbero, L.,
531 Bastos, A., Bopp, L., Ciais, P., Chini, L., Ciais, P., Doney, S., Gkritzalis, T., Goll,
532 D., Harris, I., Haverd, V., Hoffman, F., Hoppema, M., Houghton, R., Hurtt, G.,
533 Ilyina, T., Jain, A., Johannessen, T., Jones, C., Kato, E., Keeling, R., Klein
534 Goldewijk, K., Landschützer, P., Lefèvre, N., Lienert, S., Liu, Z., Lombardozzi,
535 D., Metzl, N., Munro, D., Nabel, J., Nakaoka, S. I., Neill, C., Olsen, A., Ono, T.,
536 Patra, P., Peregon, A., Peters, W., Peylin, P., Pfeil, B., Pierrot, D., Poulter, B.,
537 Rehder, G., Resplandy, L., Robertson, E., Rocher, M., Rödenbeck, C., Schuster,
538 U., Skjelvan, I., Sférian, R., Skjelvan, I., Steinhoff, T., Sutton, A., Tans, P., Tian,
539 H., Tilbrook, B., Tubiello, F., Van Der Laan-Luijkx, I., Van Der Werf, G., Viovy,
540 N., Walker, A., Wiltshire, A., Wright, R., Zaehle, S. and Zheng, B.: Global
541 Carbon Budget 2018, Earth Syst. Sci. Data, 10(4), 2141–2194,
542 <https://doi.org/10.5194/essd-10-2141-2018>, 2018.

543 Reichstein, M., Ciais, P., Papale, D., Valentini, R., Running, S., Viovy, N., Cramer, W.,
544 Granier, A., Ogée, J., Allard, V., Aubinet, M., Bernhofer, C., Buchmann, N.,
545 Carrara, A., Grünwald, T., Heimann, M., Heinesch, B., Knohl, A., Kutsch, W.,
546 Loustau, D., Manca, G., Matteucci, G., Miglietta, F., Ourcival, J. M., Pilegaard,
547 K., Pumpanen, J., Rambal, S., Schaphoff, S., Seufert, G., Soussana, J. F., Sanz,



- 548 M. J., Vesala, T. and Zhao, M.: Reduction of ecosystem productivity and
549 respiration during the European summer 2003 climate anomaly: A joint flux
550 tower, remote sensing and modelling analysis, *Glob. Chang. Biol.*, 13(3), 634–
551 651, <https://doi.org/10.1111/j.1365-2486.2006.01224.x>, 2007.
- 552 Reichstein, M., Bahn, M., Ciais, P., Frank, D., Mahecha, M. D., Seneviratne, S. I.,
553 Zscheischler, J., Beer, C., Buchmann, N., Frank, D. C., Papale, D., Rammig, A.,
554 Smith, P., Thonicke, K., Van Der Velde, M., Vicca, S., Walz, A. and Wattenbach,
555 M.: Climate extremes and the carbon cycle, *Nature*, 500(7462), 287–295,
556 <https://doi.org/10.1038/nature12350>, 2013.
- 557 Saleska, S. R., Didan, K., Huete, A. R. and Da Rocha, H. R.: Amazon forests green-up
558 during 2005 drought, *Science*, 318(5850), 612, doi:10.1126/science.1146663,
559 2007.
- 560 Sankaran, M., Hanan, N. P., Scholes, R. J., Ratnam, J., Augustine, D. J., Cade, B. S.,
561 Gignoux, J., Higgins, S. I., Le Roux, X., Ludwig, F., Ardo, J., Banyikwa, F.,
562 Bronn, A., Bucini, G., Caylor, K. K., Coughenour, M. B., Diouf, A., Ekaya, W.,
563 Feral, C. J., February, E. C., Frost, P. G. H., Hiernaux, P., Hrabar, H., Metzger, K.
564 L., Prins, H. H. T., Ringrose, S., Sea, W., Tews, J., Worden, J. and Zambatis, N.:
565 Determinants of woody cover in African savannas, *Nature*, 438(7069), 846–849,
566 <https://doi.org/10.1038/nature04070>, 2005.
- 567 Scott, R. L., Jenerette, G. D., Potts, D. L. and Huxman, T. E.: Effects of seasonal
568 drought on net carbon dioxide exchange from a woody-plant-encroached
569 semiarid grassland, *J. Geophys. Res. Biogeosciences*, 114(4), 1–13,



- 570 <https://doi.org/10.1029/2008JG000900>, 2009.
- 571 Sippel, S., Reichstein, M., Ma, X., Mahecha, M. D., Lange, H., Flach, M. and Frank,
572 D.: Drought, Heat, and the Carbon Cycle: a Review, *Curr. Clim. Chang. Reports*,
573 4(3), 266–286, <https://doi.org/10.1007/s40641-018-0103-4>, 2018.
- 574 Song, L., Luis, G., Guan, K., You, L., Huete, A., Ju, W. and Zhang, Y.: Satellite
575 sun-induced chlorophyll fluorescence detects early response of winter wheat to
576 heat stress in the Indian Indo-Gangetic Plains, *Glob. Chang. Biol.*, 24, 4023–
577 4037, <https://doi.org/10.1111/gcb.14302>, 2018.
- 578 Stocker, B. D., Zscheischler, J., Keenan, T. F., Prentice, I. C., Peñuelas, J. and
579 Seneviratne, S. I.: Quantifying soil moisture impacts on light use efficiency
580 across biomes, *New Phytol.*, 218(4), 1430–1449,
581 <https://doi.org/10.1111/nph.15123>, 2018.
- 582 Stocker, B. D., Zscheischler, J., Keenan, T. F., Prentice, I. C., Seneviratne, S. I. and
583 Peñuelas, J.: Drought impacts on terrestrial primary production underestimated
584 by satellite monitoring, *Nat. Geosci.*, 12, 274–270,
585 <https://doi.org/10.1038/s41561-019-0318-6>, 2019.
- 586 Thum, T., Aalto, T., Laurila, T., Aurela, M., Kolari, P. and Hari, P.: Parametrization of
587 two photosynthesis models at the canopy scale in a northern boreal Scots pine
588 forest, *Tellus, Ser. B Chem. Phys. Meteorol.*, 59(5), 874–890,
589 <https://doi.org/10.1111/j.1600-0889.2007.00305.x>, 2007.
- 590 Van Dijk, A. I. J. M. and Dolman, A. J.: Estimates of CO₂ uptake and release among
591 European forests based on eddy covariance data, *Glob. Chang. Biol.*, 10(9),



- 592 1445–1459, <https://doi.org/10.1111/j.1365-2486.2004.00831.x>, 2004.
- 593 Vicente-Serrano, S. M., Gouveia, C., Camarero, J. J., Beguería, S., Trigo, R.,
594 López-Moreno, J. I., Azorín-Molina, C., Pasho, E., Lorenzo-Lacruz, J., Revuelto,
595 J., Morán-Tejada, E. and Sanchez-Lorenzo, A.: Response of vegetation to
596 drought time-scales across global land biomes, *Proc. Natl. Acad. Sci. U. S. A.*,
597 110(1), 52–57, <https://doi.org/10.1073/pnas.1207068110>, 2013.
- 598 Wang, L. and Yuan, X.: Two Types of Flash Drought and Their Connections with
599 Seasonal Drought, *Adv. Atmos. Sci.*, 35(12), 1478–1490,
600 <https://doi.org/10.1007/s00376-018-8047-0>, 2018.
- 601 Wang, L., Yuan, X., Xie, Z., Wu, P. and Li, Y.: Increasing flash droughts over China
602 during the recent global warming hiatus, *Sci. Rep.*, 6, 30571,
603 <https://doi.org/10.1038/srep30571>, 2016.
- 604 Williams, C. A. and Albertson, J. D.: Soil moisture controls on canopy-scale water
605 and carbon fluxes in an African savanna, *Water Resour. Res.*, 40(9), 1–14,
606 <https://doi.org/10.1029/2004WR003208>, 2004.
- 607 Wilson, K. B., Baldocchi, D. D. and Hanson, P. J.: Quantifying stomatal and
608 non-stomatal limitations to carbon assimilation resulting from leaf aging and
609 drought in mature deciduous tree species, *Tree Physiol.*, 20, 787–797,
610 <https://doi.org/10.1093/treephys/20.12.787>, 2000.
- 611 Wolf, S., Eugster, W., Ammann, C., Häni, M., Zielis, S., Hiller, R., Stieger, J., Imer, D.,
612 Merbold, L. and Buchmann, N.: Erratum: Contrasting response of grassland
613 versus forest carbon and water fluxes to spring drought in Switzerland



- 614 (Environmental Research Letters (2013) 8 (035007)), Environ. Res. Lett., 9(8),
615 <https://doi.org/10.1088/1748-9326/9/8/089501>, 2014.
- 616 Wolf, S., Keenan, T. F., Fisher, J. B., Baldocchi, D. D., Desai, A. R., Richardson, A.
617 D., Scott, R. L., Law, B. E., Litvak, M. E. and Brunsell, N. A.: Warm spring
618 reduced carbon cycle impact of the 2012 US summer drought, 113(21),
619 5880-5885, <https://doi.org/10.1073/pnas.1519620113>, 2016.
- 620 Xie, Z., Wang, L., Jia, B. and Yuan, X.: Measuring and modeling the impact of a
621 severe drought on terrestrial ecosystem CO₂ and water fluxes in a subtropical
622 forest, J. Geophys. Res. Biogeosciences, 121(10), 2576–2587,
623 <https://doi.org/10.1002/2016JG003437>, 2016.
- 624 Xu, C., McDowell, N. G., Fisher, R. A., Wei, L., Sevanto, S., Christoffersen, B. O.,
625 Weng, E. and Middleton, R. S.: Increasing impacts of extreme droughts on
626 vegetation productivity under climate change, Nat. Clim. Chang.,
627 <https://doi.org/10.1038/s41558-019-0630-6>, 2019.
- 628 Yuan, W., Cai, W., Chen, Y., Liu, S., Dong, W., Zhang, H., Yu, G., Chen, Z., He, H.,
629 Guo, W., Liu, D., Liu, S., Xiang, W., Xie, Z., Zhao, Z. and Zhou, G.: Severe
630 summer heatwave and drought strongly reduced carbon uptake in Southern
631 China, Sci. Rep., 6, 18813, <https://doi.org/10.1038/srep18813>, 2016.
- 632 Yuan, W., Zheng, Y., Piao, S., Ciais, P., Lombardozi, D., Wang, Y., Ryu, Y., Chen, G.,
633 Dong, W., Hu, Z., Jain, A. K., Jiang, C., Kato, E., Li, S., Lienert, S., Liu, S.,
634 Nabel, J. E. M. S., Qin, Z., Quine, T., Sitch, S., Smith, W. K., Wang, F., Wu, C.,
635 Xiao, Z. and Yang, S.: Increased atmospheric vapor pressure deficit reduces



636 global vegetation growth, *Sci. Adv.*, 5(8), eaax1396,
637 <https://doi.org/10.1126/sciadv.aax1396>, 2019a.

638 Yuan, X., Ma, Z., Pan, M. and Shi, C.: Microwave remote sensing of flash droughts
639 during crop growing seasons, 17, 8196, <https://doi.org/10.1002/2015GL064125>,
640 2015.

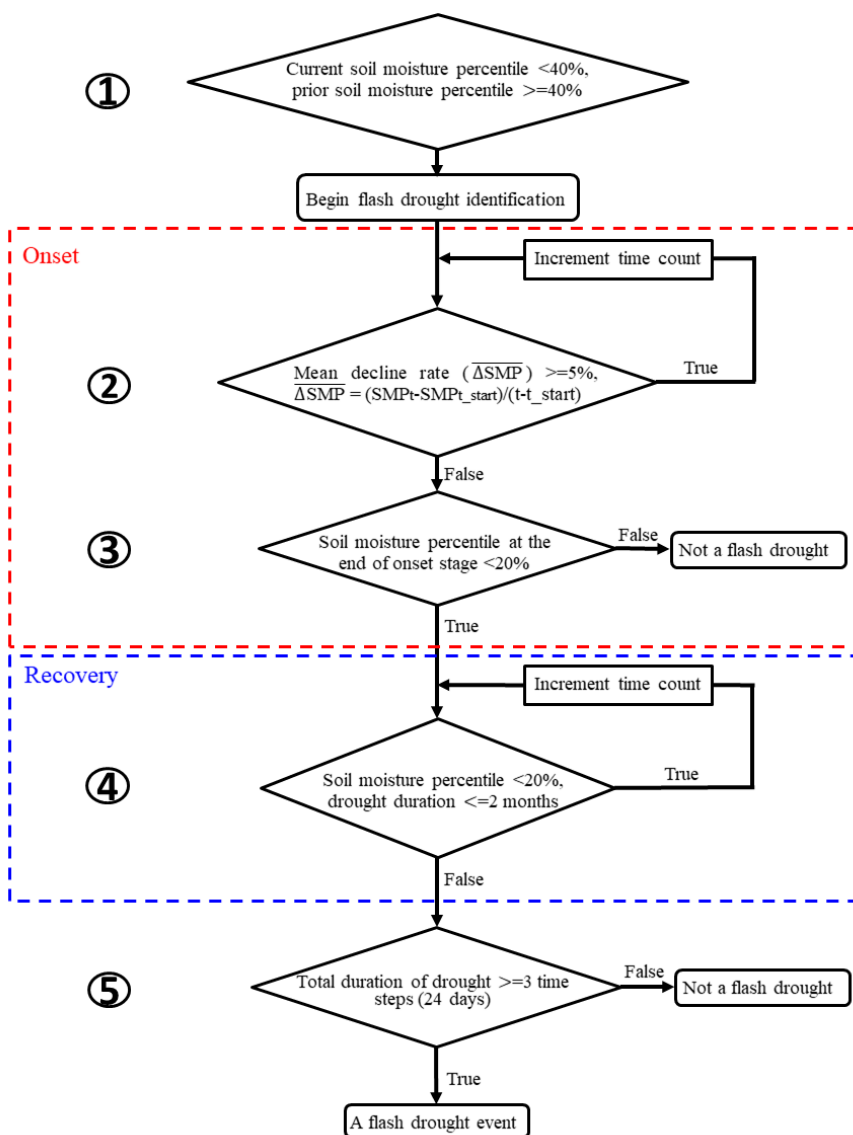
641 Yuan, X., Wang, L. and Wood, E. F.: Anthropogenic intensification of southern
642 African flash droughts as exemplified by the 2015/16 season, *Bull. Am. Meteorol.*
643 *Soc.*, <https://doi.org/10.1175/BAMS-D-17-007.1>, 2017.

644 Yuan, X., Wang, L., Wu, P., Ji, P., Sheffield, J. and Zhang, M.: Anthropogenic shift
645 towards higher risk of flash drought over China, *Nat. Commun.*, 10(1),
646 <https://doi.org/10.1038/s41467-019-12692-7>, 2019b.

647 Zeng, Z., Piao, S., Li, L. Z. X., Wang, T., Ciais, P., Lian, X., Yang, Y., Mao, J., Shi, X.
648 and Myneni, R. B.: Impact of Earth greening on the terrestrial water cycle, *J.*
649 *Clim.*, 31(7), 2633–2650, <https://doi.org/10.1175/JCLI-D-17-0236.1>, 2018.

650 Zhou, S., Yu, B., Huang, Y. and Wang, G.: The effect of vapor pressure deficit on
651 water use efficiency at the subdaily time scale, *Geophys. Res. Lett.*, 41(14),
652 5005–5013, <https://doi.org/10.1002/2014GL060741>, 2014.

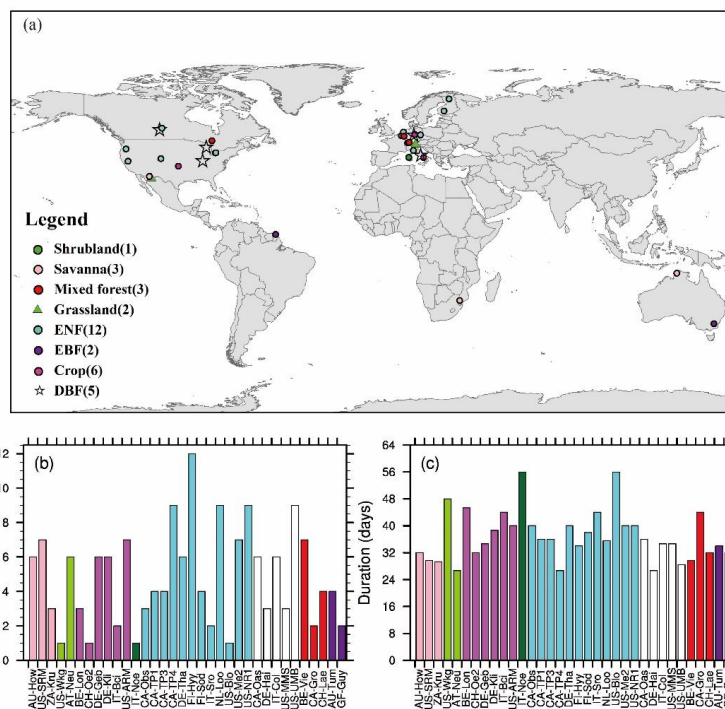
653 Zhou, S., Bofu, Y., Huang, Y. and Wang, G.: Daily underlying water use efficiency for
654 AmeriFlux sites, *J. Geophys. Res. Biogeosciences*, 120, 887–902,
655 <https://doi.org/10.1002/2015JG002947>, 2015.



656

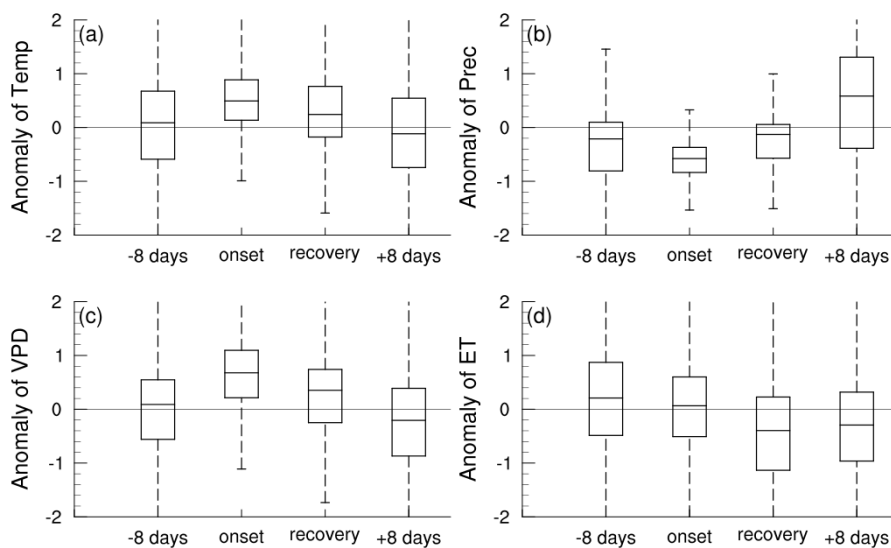
657 **Figure 1.** A flowchart of flash drought identification by considering soil moisture

658 decline rate and drought persistency.



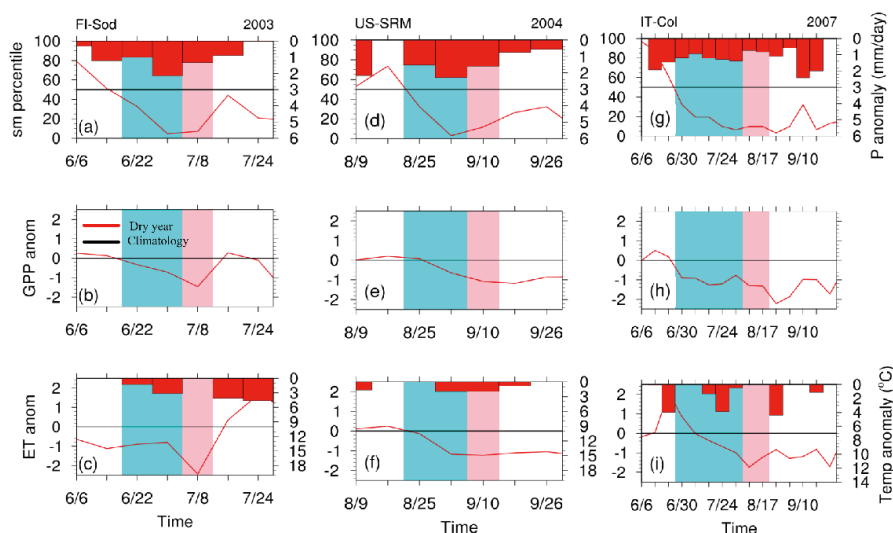
659

660 **Figure 2.** Flash drought characteristics. (a) Global map of 34 FLUXNET sites used in
661 this study. (b) Total numbers (events) and (c) mean durations (days) of flash drought
662 events for each site during their corresponding periods (see Table 1 for details).
663 Different colors represent different vegetation types.



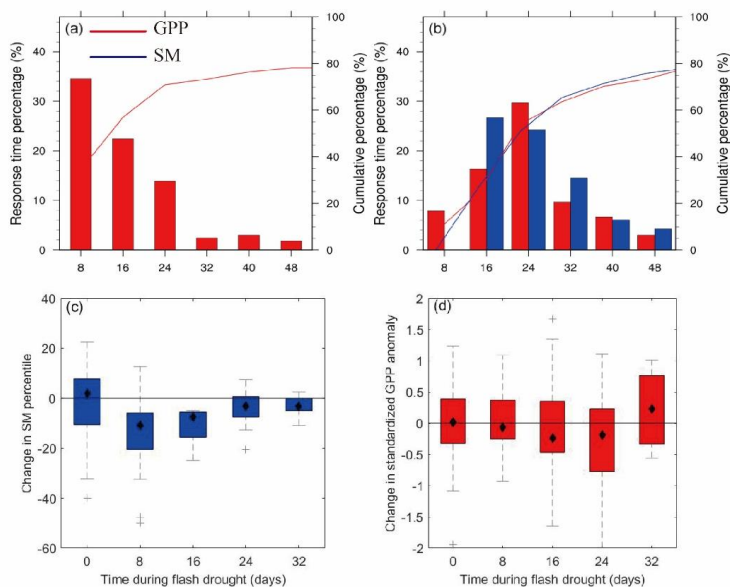
664

665 **Figure 3.** Standardized 8-day anomalies of (a) temperature, (b) precipitation, (c) VPD,
666 and (d) ET during 8 days prior to flash drought onset, onset and recovery stages of
667 flash drought, and 8 days after flash drought.



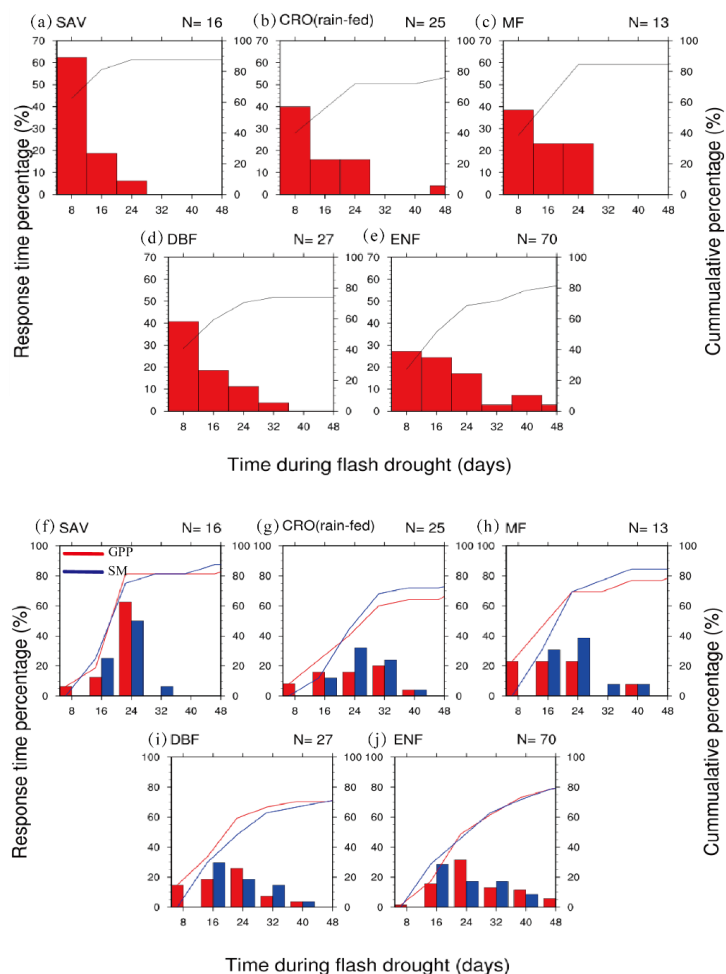
668

669 **Figure 4.** Time series of soil moisture percentile (top panels), standardized gross
670 primary productivity (GPP) anomaly (middle panels) and standardized
671 evapotranspiration (ET) anomaly (bottom panels) for the 2003 drought at FI-Sod
672 station, 2004 drought at US-SRM station and 2007 drought at IT-Col station. Red
673 lines are the time series in the target year, and black lines are the climatology
674 (long-term mean values). The red bars are precipitation deficits in top panels and
675 temperature anomalies in bottom panels, where data with positive precipitation
676 anomaly or negative temperature anomaly are not shown. The blue and pink shaded
677 areas are the onset and recovery stages of flash drought events, respectively.



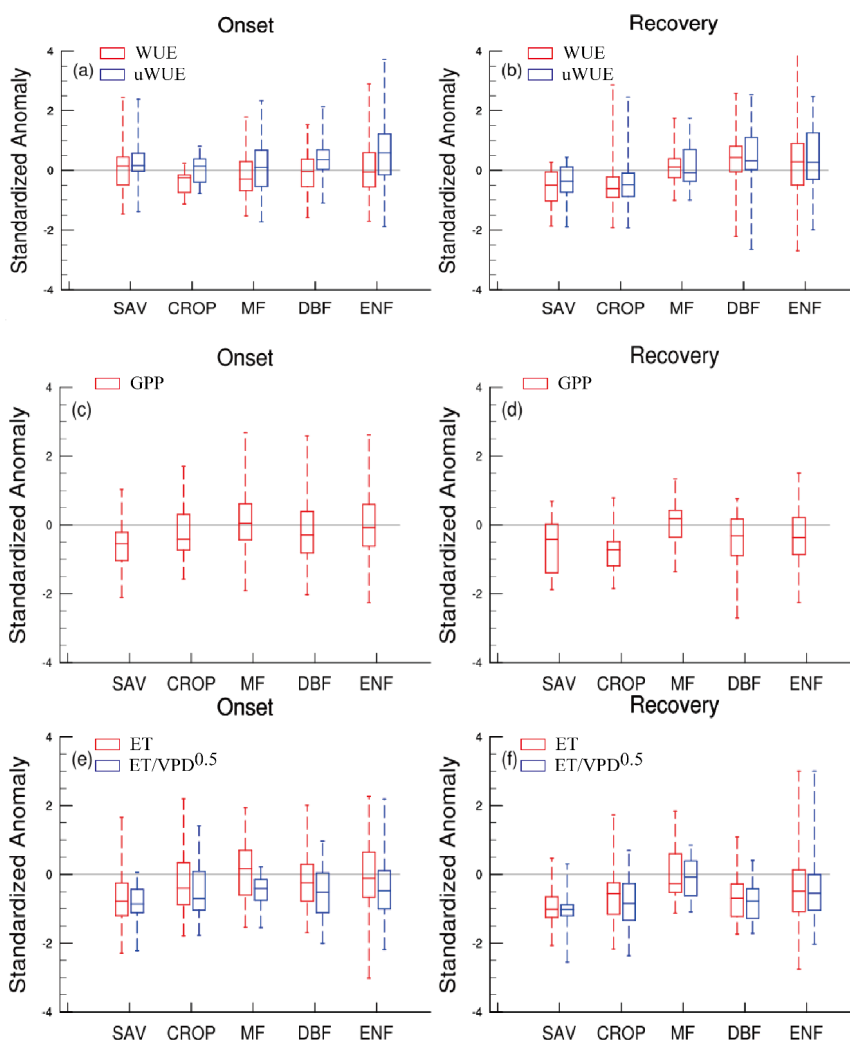
678

679 **Figure 5.** Response of carbon fluxes to flash droughts. (a) Percentage of the response
680 time of the first occurrence of negative GPP anomaly and (b) the minimum values of
681 GPP (red bars) and soil moisture (blue bars) during flash droughts. The temporal
682 change rates of (c) soil moisture percentiles and (d) standardized GPP anomalies
683 before and during flash droughts.



684

685 **Figure 6.** Percentage of the response time (days) of the first occurrence of negative
 686 GPP anomaly, minimum GPP anomaly and minimum soil moisture percentile during
 687 flash drought for different vegetation types. SAV: savanna, CRO: rainfed cropland,
 688 MF: mixed forest, DBF: deciduous broadleaf forest and ENF: evergreen needleleaf
 689 forest.



690

691 **Figure 7.** Standardized anomalies of water use efficiency (WUE), underlying WUE
692 (uWUE), GPP, ET and $ET/\sqrt{VPD}^{0.5}$ during onset and recovery stages of flash drought
693 events. SAV: savanna; CROP: cropland; MF: mixed forest; DBF: deciduous broadleaf
694 forest; ENF: evergreen needleleaf forest.

695



696 **Table 1.** Locations, vegetation types and data periods of Flux Tower Sites used in this
 697 study. WSA: woody savanna; CROP: cropland; EBF: evergreen broadleaf forests; MF:
 698 mixed forest; DBF: deciduous broadleaf forest; ENF: evergreen needleleaf forest;
 699 GRA: grassland; SAV: savanna.

station	lat	lon	IGBP	period
AT-Neu	41.12	11.32	GRA	2002-2012
AU-How	-12.49	131.15	WSA	2002-2014
AU-Tum	-35.66	148.15	EBF	2002-2014
BE-Lon	50.55	4.75	CROP-rainfed	2004-2014
BE-Vie	50.31	6.00	MF	1997-2014
CA-Gro	48.22	-82.16	MF	2004-2013
CA-Oas	53.63	-106.20	DBF	1996-2010
CA-Obs	53.99	-105.12	ENF	1999-2010
CA-TP1	42.66	-80.56	ENF	2002-2014
CA-TP3	42.71	-80.35	ENF	2002-2014
CA-TP4	42.71	-80.36	ENF	2002-2014
CH-Lae	47.48	8.37	MF	2005-2014
CH-Oe2	47.29	7.73	CROP-rainfed	2004-2014
DE-Geb	51.10	10.91	CROP-rainfed	2001-2014
DE-Hai	51.08	10.45	DBF	2000-2012
DE-Kli	50.89	13.52	CROP-rainfed	2005-2014
DE-Tha	50.96	13.57	ENF	1997-2014
FI-Hyy	61.85	24.29	ENF	1997-2014
FI-Sod	67.36	26.64	ENF	2001-2014
GF-Guy	5.28	-52.92	EBF	2004-2014
IT-Bci	40.52	14.96	CROP-irrigated	2005-2014
IT-Col	41.85	13.59	DBF	2005-2014
IT-Noe	40.61	8.15	SH	2004-2014
IT-Sro	43.73	10.28	ENF	2000-2012
NL-Loo	52.17	5.74	ENF	1999-2013
US-ARM	36.61	-97.49	CROP-rainfed	2003-2013
US-Blo	38.90	-120.63	ENF	1998-2007
US-Me2	44.45	-121.56	ENF	2002-2014
US-MMS	39.32	-86.41	DBF	1999-2014
US-NR1	40.03	-105.55	ENF	2002-2014
US-SRM	31.82	-110.87	WSA	2004-2014
US-UMB	45.56	-84.71	DBF	2002-2014
US-Wkg	31.74	-109.94	GRA	2005-2014
ZA-Kru	-25.02	31.50	SAV	2000-2010